Proc. Natl. Acad. Sci. USA
Vol. 88, pp. 11129–11132, December 1991
Applied Mathematics

Predicting chaos for infinite dimensional dynamical systems: The Kuramoto–Sivashinsky equation, a case study

YIORGOS S. SMYRLIS[†] AND DEMETRIOS T. PAPAGEORGIOU[‡§]

[†]Department of Mathematics, University of California at Los Angeles, Los Angeles, CA 90024-1555; and [‡]Department of Mathematics, New Jersey Institute of Technology, Newark, NJ 07102

Communicated by Peter D. Lax, July 25, 1991

ABSTRACT **The results of extensive computations are presented to accurately characterize transitions to chaos for the Kuramoto–Sivashinsky equation. In particular we follow the oscillatory dynamics in a window that supports a complete sequence of period doubling bifurcations preceding chaos. As many as 13 period doublings are followed and used to compute the Feigenbaum number for the cascade and so enable an accurate numerical evaluation of the theory of universal behavior of nonlinear systems, for an infinite dimensional dynamical system. Furthermore, the dynamics at the threshold of chaos exhibit a self-similar behavior that is demonstrated and used to compute a universal scaling factor, which arises also from the theory of nonlinear maps and can enable continuation of the solution into a chaotic regime. Aperiodic solutions alternate with periodic ones after chaos sets in, and we show the existence of a period six solution separated by chaotic regions.**

1. Introduction

A central question in fluid dynamics that is attracting a considerable research effort is the prediction of onset to turbulence. A general theory encompassing the Navier–Stokes equations of fluid motion, and consequently covering a large class of physical phenomena, is not available at present. As a result most contributions are focused on the analysis of model equations derived from the Navier–Stokes system by asymptotic methods, for example, or by finite-dimensional truncations (1). In many cases this is a valid and useful approach, especially in the light of Feigenbaum's fascinating theory originally for one-dimensional nonlinear maps (2–4), which predicts universal nonlinear behavior and is believed to be applicable to many more complex nonlinear systems such as ordinary and partial differential equations. A brief review of Feigenbaum's theory for the quadratic map is in order here, but the interested reader should refer to the above mentioned articles (also ref. 5). The theory pertains to one-parameter families of mappings of an interval onto itself, a representative example of which is

$$f(x) = 4\nu x(1-x), \quad 0 \le \nu \le 1, \quad x \in [0, 1]. \qquad [1]$$

The flow is obtained by repeated application of Eq. **1**. $x = 0$ is a fixed point of each member of the family (1). For $0 < \nu \le 1/4$, $x = 0$ is the only fixed point and it is globally attractive—i.e., the iterates of f, starting at any x in [0, 1], converge to $x = 0$. For $1/4 < \nu < 1$, another fixed point appears at $x = 1 - 1/4\nu$, and it is globally attractive for $1/4 < \nu \le 3/4$. At $\nu = 3/4$ the fixed point becomes unstable and bifurcates into two fixed points, x_{11} and x_{12}, of the twice iterated map $f(f(x)) = f^2(x)$ with $f(x_{11}) = x_{12}$ and $f(x_{12}) = x_{11}$. This period 2 cycle is globally attractive for all sequences of iterates in the range $3/4 < \nu < \nu_2$. At ν_2 the 2-cycle becomes unstable, a 4-cycle consisting of fixed points of f^4 emerges that is globally attractive in a range $\nu_2 < \nu < \nu_3$, and so *ad infinitum*. The sequence of values ν_n at which a period doubling occurs tend to a limiting value $\nu_\infty < 1$; for $\nu_\infty < \nu < 1$, the flow is mostly chaotic. The rate at which the ν_n approach ν_∞ is geometric, and the limiting ratio

$$\delta = \lim_{n\to\infty} \frac{\nu_n - \nu_{n-1}}{\nu_{n+1} - \nu_n} = 4.6692016\ldots \qquad [2]$$

is the same for all one-parameter families of unimodal C^2 mappings of [0, 1] whose maxima are nondegenerate—i.e., $f'' \neq 0$. The constant δ is called the Feigenbaum number.

There is another universal constant we compute here. Take a stable 2^{n+1} cycle and arrange its x coordinates in increasing order: $x_1 < x_2 < \cdots < x_{2^{n+1}}$. Consider now the lower half of this sequence, S_1 say, with $x_1 < x_2 < \cdots < x_{2^n} < x*$ where $x*$ is the unstable fixed point of Eq. **1**. Rescale the upper half of S_1, S_2 say, $x_{2^{n-1}+1} < \cdots < x_{2^n}$, to the same size as S_1 by a factor $\alpha_1 = \dfrac{x_{2^n} - x_1}{x_{2^n} - x_{2^{n-1}+1}}$. Next rescale the lower half of S_2, S_3 say, $x_{2^{n-1}+1} < \cdots < x_{2^{n-1}+2^{n-2}}$ to the same size as S_2 by a factor $\alpha_2 = \dfrac{x_{2^n} - x_{2^{n-1}+1}}{x_{2^{n-1}+2^{n-2}} - x_{2^{n-1}+1}}$. Next, the upper half of S_3, S_4 say, $x_{2^{n-1}+2^{n-3}+1} < \cdots < x_{2^{n-1}+2^{n-2}}$ is rescaled to the same size as S_3 by a factor $\alpha_4 = \dfrac{x_{2^{n-1}+2^{n-2}} - x_{2^{n-1}+1}}{x_{2^{n-1}+2^{n-2}} - x_{2^{n-1}+2^{n-3}+1}}$, and so on. Feigenbaum (2–4) has observed that for fixed n, the factors α_i $i = 1, \ldots, n-2$ converge very rapidly, and as $n \to \infty$, the converged value is $\alpha = 2.502907875\ldots$. This constant too is universal in the class of unimodal nondegenerate C^2 maps of [0, 1].

Feigenbaum predicted such universal behavior for continuous time flows of infinite dimensional (continuum) systems. He has (7) observed such self-similarity in experiments with Rayleigh–Benard flows. In this paper we describe carefully computed numerical solutions of the Kuramoto–Sivashinsky equation that clearly display period doublings, as many as 13 of them, and universal behaviors: the continuum analogues of both universal constants δ and α, when computed from our numerical data, agree with the values of the one-dimensional theory to 3 decimals.

The equation studied, the Kuramoto–Sivashinsky equation, can be written in the form

$$u_t + uu_x + u_{xx} + \nu u_{xxxx} = 0,$$

$$(x, t) \in \mathbf{R}^1 \times \mathbf{R}^+,$$

$$u(x, 0) = u_0(x), \quad u(x + 2\pi, t) = u(x, t), \qquad [3]$$

The publication costs of this article were defrayed in part by page charge payment. This article must therefore be hereby marked "*advertisement*" in accordance with 18 U.S.C. §1734 solely to indicate this fact.

[§]To whom reprint requests should be addressed.

Table 1. Overview of the most attracting manifolds

Window range	Description of the attractors
$1 \leq \nu < \infty$	Trivial solution
$0.25 \leq \nu < 1$	Steady state of period 2π
$0.0756 < \nu < 0.025$	Steady state of period π
$0.06697 \leq \nu \leq 0.0755$	Steady state of period 2π
$0.05992 \leq \nu \leq 0.06695$	Steady state of period $2\pi/3$
$0.05516 \leq \nu \leq 0.05991$	Time periodic attractor
$0.0396227 \leq \nu \leq 0.05515$	Steady state of period 2π
$0.03729 \leq \nu \leq 0.0396226$	Time periodic attractor
$0.0346259 \leq \nu \leq 0.03728$	Steady state of period $\pi/2$
$0.029969103484 \leq \nu \leq 0.0346258$	Time periodic attractor containing complete period-doubling sequence
$0.02922 \leq \nu \leq 0.02969910348$	Chaotic oscillations
$0.02905 \leq \nu \leq 0.02921$	Time periodic attractor
$0.02855 \leq \nu \leq 0.02904$	Chaotic oscillations
$0.02662 \leq \nu \leq 0.02854$	Time periodic attractor
$0.02525 \leq \nu \leq 0.02661$	Chaotic oscillations
$0.02506 \leq \nu \leq 0.02524$	Time periodic attractor
$0.0248607 \leq \nu \leq 0.02505$	Chaotic oscillations
$0.02445 \leq \nu \leq 0.0248606$	Time periodic attractor containing complete period-doubling sequence
$0.0242861 \leq \nu \leq 0.02445$	Chaotic oscillations
$0.02367 \leq \nu \leq 0.02438608$	Time periodic attractor containing complete period-doubling sequence
$0.0232 \leq \nu \leq 0.02386$	Chaotic oscillations
$0.0229 \leq \nu \leq 0.0231$	Time periodic attractor
$0.0223 \leq \nu \leq 0.0228$	Chaotic oscillations
$0.022 \leq \nu \leq 0.0222$	Time periodic attractor
$? \leq \nu \leq 0.0219$	Chaotic oscillations

where $\nu > 0$ is the viscosity of the system. This equation arises in a variety of problems such as concentration waves (8), flame propagation (9), free surface flows (10). A generalized form, of which Eq. 3 is a special case, has been derived by an asymptotic analysis of the Navier–Stokes equations in the context of two-phase flows in cylindrical geometries with applications in lubricated pipe-lining (for the efficient transport of crude oil) and oil recovery through porous media (11). Much analytical and computational work has been completed to describe the complicated nonlinear dynamics that Eq. 3 can produce as ν varies and, in particular, when it achieves fairly small values (see refs. 12 and 13).

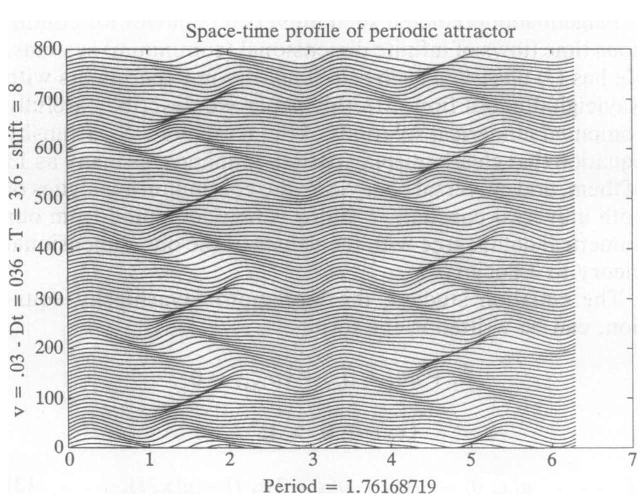

FIG. 1. Spatio-temporal evolution at $\nu = 0.03$. Solution has undergone two period doublings and is *en route* to chaos.

Table 2. Computation of the Feigenbaum number

Subwindow boundary ν	Subwindow length	Ratio of lengths	Time period
0.0346258	4.3083×10^{-3}	—	0.44
0.03031749	2.6825×10^{-4}	—	0.88
0.030049233	6.2786×10^{-5}	16.061	1.76
0.029986446	1.3609×10^{-5}	4.2724	3.52
0.0299728366	2.9330×10^{-6}	4.6136	7.03
0.0299699036	6.288×10^{-7}	4.6399	14.05
0.02996927484	1.3456×10^{-7}	4.6644	28.1
0.02996914018	2.884×10^{-8}	4.6657	56.2
0.02996911134	6.18×10^{-9}	4.667	112.4
0.02996910516	1.32×10^{-9}	4.68	224.8
0.029969103842	2.84×10^{-10}	4.65	449.6
0.029969103558	6.0×10^{-11}	4.7	899.1
0.029969103498	1.4×10^{-11}	4.	1798.2
0.029969103484		—	∞

2. Numerical solutions.

The results presented here were obtained by numerical solution of the initial value problem (Eq. 3) with the initial condition

$$u_0(x) = -\sin(x),$$

for all values of ν. Since solutions of Eq. 3 are uniquely determined by their initial data, a solution that is an odd function of x initially will remain so for all subsequent times. The advantage of such a choice is that there exist analytical results that give global bounds for $u(x, t)$ and higher derivatives in the odd-parity case (14); the bounds available in the general case grow exponentially in t (15). The numerical scheme is a Galerkin spectral method based on a sine series

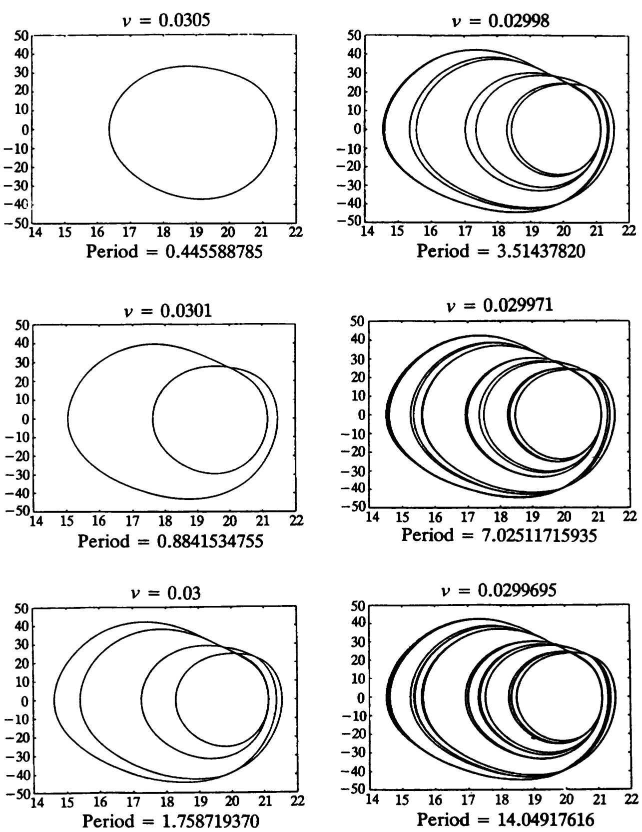

FIG. 2. The phase plane showing the first five period doublings. The values of ν are given on the figure as well as the time periods.

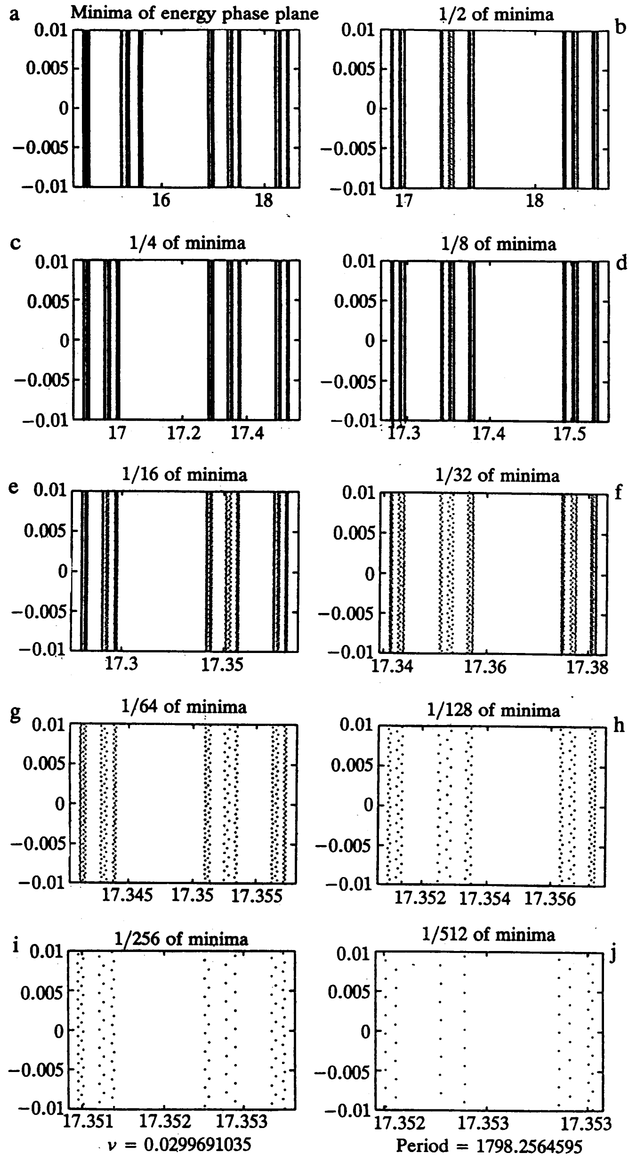

FIG. 3. Successive magnification of the energy minima of the 2^{12}-cycle, showing the self-similar characteristics of the attractor.

and is described in detail in ref. 12. The truncation order of the Galerkin approximation depends on the value of ν; a crude estimate that has proven practical shows that it suffices to retain a few frequencies more than $\nu^{-1/2}$, the number of linearly unstable ones around $u = 0$. Taking any more frequencies does not change the computed solution; this number is an upper bound on the dimension of the attractor. In ref. 16 it was shown that the Hausdorff dimension of the attractor does not exceed *const* $\nu^{-21/40}$, which is larger than $\nu^{-1/2}$ by a factor of *const* $\nu^{-1/40}$; the constant, however, is very large.

Since the Kuramoto–Sivashinsky equation (Eq. 3) is in conservative form, $\int_0^{2\pi} u(x, t)dx$ is a conserved quantity. It has been proved that when $\nu > 1$, every solution whose integral is zero initially tends to zero uniformly; this is borne out by our numerical calculations. As we decrease ν below 1, the zero solution becomes unstable, bifurcates, and tends for large t to a steady nonconstant state. When ν decreases below 1/4, u tends to a new linearly stable steady state whose spatial period is π. Further decrease of ν gives stable steady states of spatial period 2π and $2\pi/3$. At $\nu = 0.05991$, a time-periodic attractor is found; a single period doubling occurs in this

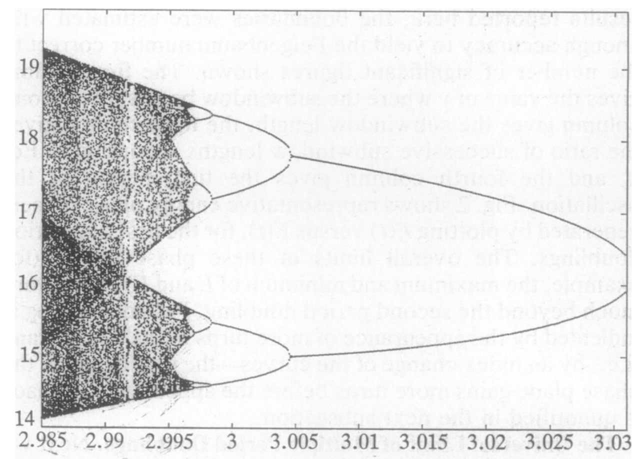

FIG. 4. Route to chaos and beyond for the minima of the energy of the Kuramoto–Sivashinsky equation. Disorder sets in as the viscosity ν decreases from right to left. The ν axis has been enlarged by a factor of 100.

window (by window we mean intervals of ν that attract qualitatively similar solutions), but as ν is decreased further, the solutions are attracted to steady states of spatial period 2π. Next we find a new time-periodic window with two period doublings and one period halving. Further decrease of ν gives steady states with spatial period $\pi/2$. Next we find a third periodic window that contains a complete sequence of period-doubling bifurcations (we could identify 13), which lead to chaos, and so on (see Table 1).

A graphical view of the solutions at $\nu = 0.03$ is presented in Fig. 1. The time period here is 1.76168719, and we are in the subwindow directly after the second period-doubling. The spatial and temporal evolution of the profile are collectively shown over a domain $x \in [0, 2\pi]$ with u on the vertical axis and x on the horizontal axis. One hundred profiles are plotted at time intervals of 0.036 and shifted vertically by a distance of 8 units. The whole duration of the picture is 3.6 time units and contains approximately two time periods.

Computation of the Feigenbaum Number. Table 2 presents our evidence that verifies Feigenbaum's universal theory for the Kuramoto–Sivashinsky equation. These results were generated by monitoring the evolution of the energy, $E(t)$—i.e., the L^2-norm of the solution. Each entry in Table 2 represents the beginning of successive subwindows, which support solutions that undergo period doublings. The sharp estimation of these boundaries is necessary if an accurate computation of the Feigenbaum number is desired. In all

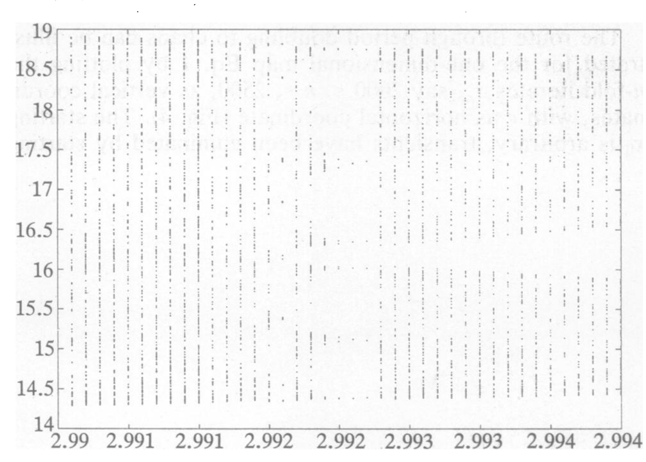

FIG. 5. Enlargement of Fig. 4 route to chaos for the minima of the energy of the Kuramoto–Sivashinsky equation. The 6-cycle solution is seen between 2.992 and 2.993.

results reported here, the boundaries were estimated with enough accuracy to yield the Feigenbaum number correct to the number of significant figures shown. The first column gives the value of ν where the subwindow begins, the second column gives the subwindow length, the third column gives the ratio of successive subwindow lengths according to Eq. 2, and the fourth column gives the time period of the oscillation. Fig. 2 shows representative energy phase planes, generated by plotting $E(t)$ versus $\dot{E}(t)$, for the first five period doublings. The overall limits of these phase planes (for example, the maximum and minimum of E and $\dot{E}$) do not vary much beyond the second period doubling. Period doubling is indicated by the appearance of more turns in the phase plane (i.e., by an index change of the curves—the way in which the phase plane gains more turns before the appearance of chaos is quantified in the next subsection.

The Universal Limit of Multiple Period Doublings. Next we present a set of numerical results that exhibit very clearly the self-similar nature of period-doubling bifurcations. The experiment we choose has a value of $\nu = 0.0299691035$ and lies at the end of the third periodic window; at a value of $\nu = 0.029969103484$—i.e., a decrease of 1.6×10^{-11}—chaotic solutions are observed. The time period of the solution is 1798.2564595 units and is the result of a sequence of 12 period doublings (in Fig. 1 we show only the first 5). The energy $E(t)$ of this solution is a scalar-valued periodic function; because of the 12 period doublings, it has 2^{11} local minima in one period. We arrange these in increasing order $E_1 < E_2 < \cdots < E_{2^{11}}$. In Fig. 3*a*, we picture these values by drawing a vertical line through each E_i, $i = 1, \ldots, 2^{11}$. In Fig. 3*b* we picture the upper half of these energy minima $E_i, i = 2^{10} + 1, \ldots, 2^{11}$, rescaled to the same size by the factor $\alpha_1 = \dfrac{E_{2^{11}} - E_1}{E_{2^{11}} - E_{2^{10}+1}}$. In Fig. 3*c* we depict the lower half of the sequence in Fig. 3*b*, E_i, $i = 2^{10} + 1, \ldots, 2^{10} + 2^9$, rescaled to the same size by a factor $\alpha_2 = \dfrac{E_{2^{11}} - E_{2^{10}+1}}{E_{2^{10}+2^9} - E_{2^{10}+1}}$. In Fig. 3*d* we picture the upper half of the sequence in Fig. 3*c*, E_i, $i = 2^{10} + 2^8 + 1, \ldots, 2^{10} + 2^9$, rescaled by a factor $\alpha_3 = \dfrac{E_{2^{10}+2^9} - E_{2^{10}+1}}{E_{2^{10}+2^9} - E_{2^{10}+2^8+1}}$. We repeat this procedure noting the remaining enlargement factors $\alpha_4, \ldots, \alpha_9$. The self-similar structure of the attractor is clearly seen from these figures. The scale factors α_i converge very rapidly to the value 2.503, in very good agreement with Feigenbaum's second universal constant $\alpha = 2.502907875\ldots$. These results provide another instance of complete confirmation of Feigenbaum's universal theory for the Kuramoto–Sivashinsky equation.

The route through period doubling to chaos can be illustrated for the one-dimensional map Eq. 1 by plotting the n-fold iterates x_n, say $2000 < n < 2500$, as vertical coordinates, with ν as horizontal coordinate (Fig. 4). The starting x_0 is arbitrary; transients have been eliminated by starting with the 2000th iterate. A 2-cycle at a parameter value ν will appear as two dots, a 4-cycle at a different value of ν as four dots and so on. The final picture produced is the locus of all such points as ν varies between 0 and 1.

For the Kuramoto–Sivashinsky equation an analogous picture can be constructed, as follows. We begin with the first subwindow where the solution first becomes periodic. For a range of ν we plot as vertical coordinates the minima of the energy $E(t)$ of the solution $u(x,t)$ in the time interval, say $60 < t < 120$, to eliminate transients, with ν as horizontal coordinate. As ν crosses subwindow boundaries and the solution attains a period doubling, the number of minima doubles. Chaos sets in as ν decreases, and the solution is clearly seen to attain several period doublings before an accumulation point is reached; below the accumulation point chaos sets in and appears by the irregular positioning of the minima (dots). Most interestingly, however, our computations show a region in the interval $[2.99, 2.995] \times 10^{-2}$ where we observe 6-cycle solutions. An enlargement of this region is given in Fig. 5. The alternating between aperiodic and periodic attractors in the region beyond the accumulation point is fairly typical of numerical experiments on one-dimensional maps. Our results indicate that this behavior is also supported by infinite-dimensional continuum systems.

The authors express their deepest thanks to Professor P. D. Lax for taking an interest in this work and for many constructive comments regarding the manuscript. We also thank Professors G. C. Papanicolaou and S. Osher for many useful discussions. This research was supported in part by the National Aeronautics and Space Administration (NASA) under Contract NAS1-18605 while the authors were in residence at ICASE, NASA Langley Research Center, Hampton, VA. Additional support to Y.S.S. was provided by Office of Naval Research Grant N-00014-86-K-0691 at UCLA.

1. Lorenz, E. N. (1963) *J. Atmos. Sci.* **20**, 130–141.
2. Feigenbaum, M. J. (1977) *Universality in Complex Discrete Dynamical Systems* (Los Alamos Natl. Lab., Los Alamos, NM), Tech. Rep. LA-6816-PR, pp. 98–102.
3. Feigenbaum, M. J. (1978) *J. Stat. Phys.* **19**, 25–52.
4. Feigenbaum, M. J. (1978) *J. Stat. Phys.* **21**, 669–706.
5. Collet, P. & Eckman, J. P. (1980) *Iterated Maps of the Interval as Dynamical Systems* (Birkhauser, Boston).
6. Feigenbaum, M. J. (1983) *Physica D* **7**, 16–39.
7. Feigenbaum, M. J. (1979) *Phys. Lett. A* **74**, 375–378.
8. Kuramoto, Y. (1978) *Suppl. Prog. Theor. Phys.* **64**, 346–367.
9. Sivashinsky, G. I. (1977) *Acta Astron.* **4**, 1176–1206.
10. Benney, D. J. (1966) *J. Math. Phys.* **45**, 150–155.
11. Papageorgiou, D. T., Maldarelli, C. & Rumschitzki, D. S. (1990) *Phys. Fluids A* **2**, 340–352.
12. Papageorgiou, D. T. & Smyrlis, Y. S. (1991) *Theor. Comput. Fluid Dyn.* **3**, 15–42.
13. Jolly, M. S., Kevrekides, I. G. & Titi, E. S. (1990) *Physica D* **44**, 38–60.
14. Nicolaenko, B., Scheurer, B. & Temam, R. (1985) *Physica D* **16**, 155–183.
15. Tadmor, E. (1986) *SIAM J. Appl. Math.* **17**, 884–893.
16. Foias, C., Nicolaenko, B., Sell, G. R. & Temam, R. (1988) *J. Math. Pures Appl.* **67**, 197–226.